Interactive Simulation of Disease Contagion in Dynamic Crowds

Alon Flor*
Chengguizi Han*
Tao Xue*
af656@cs.rutgers.edu
chengguizi.han@rutgers.edu
tx57@cs.rutgers.edu
Rutgers, The State University of New Jersey
Piscataway, NJ 08854, United States of America

Mridul Aanjaneya
ma635@cs.rutgers.edu
Rutgers, The State University of New Jersey
Piscataway, NJ 08854, United States of America

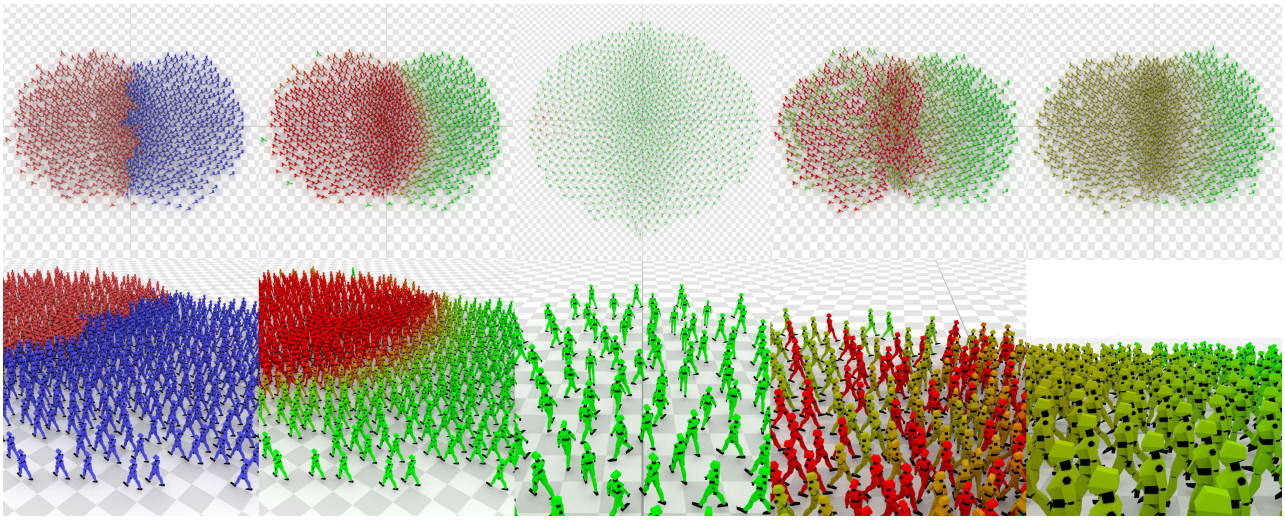

From left to right: Crowd interaction, Unprotected, Social distancing, Immunity, and Vaccination.

Figure 1: Our novel disease spreading model at the agent-to-agent scale provides specific information about the infectivity within moving crowds, and also supports different health interventions. The number of infected people is significantly small in crowds with social distancing and vaccination. The infectivity is visualized with colors from green (low) to red (high).

ABSTRACT

We propose an agent-to-agent contagion-immunity formulation that can simulate detailed COVID-19 spreading within moving crowds. Specifically, we develop a diffusion-based disease contagion model for discrete systems that considers the effect of health interventions, such as social distancing, immunity, and vaccination. We integrate our contagion-immunity formulation with the governing equations of motion for crowd dynamics for investigating the distribution of disease in crowds with different numbers of people. For the same crowd simulation, our model can interactively simulate virus spread for different initial distributions of infected people. To the best of our knowledge, our work is the first to simulate the disease contagion within moving crowds in computer graphics. Our numerical results for the number of infected people in unprotected dense crowds agree with the SIS model, while our model provides richer information for disease spread and shows that vaccination is the best health intervention to prevent infection.

*Joint first authors.

MIG'21, November 10–12, 2021, Lausanne, Switzerland

ACM ISBN 978-1-4503-9131-3/21/11…$15.00
https://doi.org/10.1145/3487983.3488298

CCS CONCEPTS

• **Computing methodologies** → *Computer graphics*; Physical simulation.

KEYWORDS

disease spreading models, crowd simulation, contagion-immunity interaction, discrete diffusion modeling

ACM Reference Format:
Alon Flor, Chengguizi Han, Tao Xue, and Mridul Aanjaneya. 2021. Interactive Simulation of Disease Contagion in Dynamic Crowds. In *MIG'21: Motion, Interaction and Games.* ACM, New York, NY, USA, 11 pages. https://doi.org/10.1145/3487983.3488298

1 INTRODUCTION

Over the last two years, we have experienced the historic, global outbreak of Coronavirus Disease 2019 (COVID-19) which, along with the measures taken to mitigate it, have struck at everyday life worldwide [Bock et al. 2020; Chowdhury et al. 2020; Walker et al. 2020]. Each country had to find its own way to keep the rapid virus spread under control, to "flatten the curve", and to avoid a breakdown of its healthcare system. The main strategies recommended by epidemiologists are wearing masks and maintaining social distancing. Recently, with the successful development of COVID-19 vaccines, getting vaccinated has been added to the list [Cartaud et al. 2020; Qian and Jiang 2020; Xu and Cheng 2021].

To date, numerous mathematical studies have focused on modeling the outbreak dynamics of COVID-19, predicting its future course, and providing scientific reasoning for political decisions. Traditional epidemiology models represent epidemics of communicable diseases using a population-based, non-spatial approach [Bian 2004]. The conceptual framework for this approach is rooted in the general population model which divides a population into different segments [Kermack and McKendrick 1927], including Susceptible, Infected, and Removed (SIR), among others, and formulates their coupled evolution with a set of ordinary differential equations (ODEs). These SIR-based deterministic models [Comunian et al. 2020; Conejero et al. 2019; Ehrhardt et al. 2019; Giudici et al. 2020] assume that populations are completely mixed and ignore the spatial effects involved in the spread of epidemics. These models also neglect the interactions between individuals since they model populations as continuous entities [Di Stefano et al. 2000].

In contrast to SIR-based epidemic simulations, *agent*-based formulations [Connell et al. 2009; Newman 2002; Perez and Dragicevic 2009] are stochastic and spatially explicit, permitting the modeller to study specific spatial aspects of the spread of epidemics. Modeling in epidemiology using an agent-based approach pursues the progression of a disease through each individual, and tracks the contacts of each individual with others in the relevant social networks and geographical areas (e.g., co-workers, schoolmates). Thus, populations become highly heterogeneous by health status during simulations. All the rules for individual agent movement (e.g., to and from workplace and/or school) and for contacts with and transmissions to other people are explicit [Epstein et al. 2012; Salam et al. 2021]. Moreover, agent-based models can produce emergent macro-effects from micro-rules and have played an important role in the development of different methodological frameworks in epidemiology [Connell et al. 2009]. However, the disease spreading model embedded in the dynamical interaction among agents still relies heavily upon the SIR-based model, which only depicts the statistical characteristics of disease spreading, such as the percentage of infected population members. The specific infectivity of each individual agent in real-life scenarios, such as concerts, football games, and parades, appears to be impossible to regain from the prior agent-based simulations with SIR-based disease spreading (see Section 2.3 for more details).

According to the latest epidemic report[1], COVID-19 is recognized to be a highly contagious disease, and regular gatherings and events, such as in supermarkets, schools, and concerts, appear to be dangerous activities that may lead to a massive increase in the number of infected people. Therefore, instead of studying the disease spreading over a large domain, such as globally, it appears to be more vital to investigate the disease spreading pattern within a limited domain where the individuals can be modelled directly.

In this paper, we propose a novel disease spreading model at the *agent-to-agent* scale and investigate the COVID-19 spreading in a moving crowd. Our disease spreading model starts from a discrete diffusion process [Wang et al. 2016; Xue et al. 2019], demonstrating the disease transmission from one agent to its neighboring agents. We consider the disease as a "predator" and the inner immune systems of agents as "prey", and use the *predator-prey relationship to describe the general loss-win interactions between infectivity and immunity*. Our agent-to-agent based contagion-immunity formulation integrates agent-based discrete crowd simulation [Jiang et al. 2010; Kolivand et al. 2021; Narain et al. 2009], the *predator-prey* equation [Berryman 1992; Chattopadhyay and Arino 1999], and discrete diffusion modeling [Wang et al. 2016; Xue et al. 2019], provides specific information about how risky these mass events can be, and supports the recommended intervention measures (i.e., wearing masks, social distancing, and getting vaccinated). In summary, our main contributions are as follows:

(1) An agent-to-agent contagion-immunity formulation that provides detailed COVID-19 spreading within moving crowds.
(2) End-to-end simulations with social distancing, immunity, and vaccination to highlight the versatility of our method.

2 RELATED WORK

2.1 Crowd Simulation

Simulations of virtual crowds have been extensively studied in several fields, including computer graphics, robotics, traffic engineering, and social sciences. We refer the readers to excellent surveys [Pelechano et al. 2008; Thalmann et al. 2007].

In the present work, we utilize collision avoidance algorithms to simulate crowds. Collision avoidance algorithms can be generally classified into continuum and discrete approaches. Continuum approaches formulate the dynamics of crowds based on *continuum mechanics*, and the behavior of pedestrians presents fluid-like behavior. The governing equations of these continuum approaches are usually *partial differential equations* (PDEs) that involve equations for density and mean velocity of the flow, and are particularly suitable for dense, homogeneous crowds and complex environments [Bellomo and Dogbe 2011; Etikyala et al. 2014; Helbing 1998].

On the contrary, discrete approaches simulate individuals and the crowds that naturally form by agent interactions, in which agents are usually approximated by disks. Most collision-avoidance algorithms for agent-based simulations are based on social forces [Helbing and Molnar 1995; Kang et al. 2019], velocity selection [Kim et al. 2015; Van den Berg et al. 2008] or vision [Dutra et al. 2017],

[1] https://www.cdc.gov/coronavirus/2019-ncov/community/large-events/considerations-for-events-gatherings.html

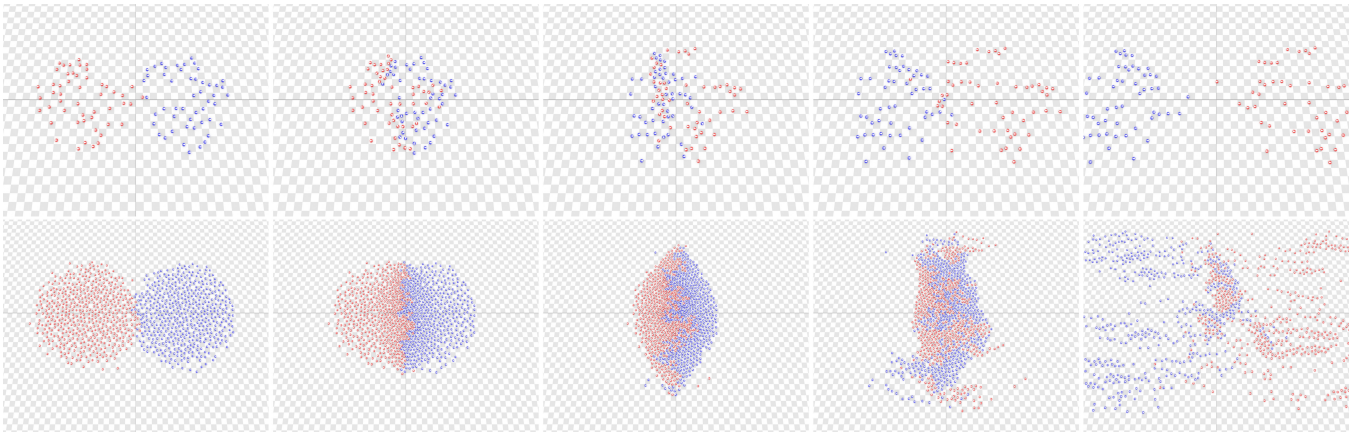

Figure 2: Crowd simulations. Top: sparse passing. Bottom: dense passing. Our simulations capture group interactions in both the sparse and dense passing scenarios, and they agree with other position-based crowd simulations [Weiss et al. 2019].

and the influence of emotion evolution/contagion [Jiang et al. 2018; Xu et al. 2019]. To enhance the agent-based model, Kim et al. [2015] have added detailed physical interaction forces (such as pushing) to simulate a crowded pilgrimage scenario. Hesham and Wainer [2021] have given agents a dynamic personal space that adapts to their current speed. Smoothed Particle Hydrodynamics (SPH) [van Toll et al. 2021] has been integrated with the agent-based force to allow agents to blend between individual navigation and fluid-like interactions depending on the SPH density. Position-Based Dynamics (PBD) [Weiss et al. 2019] has also been applied for crowd simulations. In the present work, we use the simple social force formulation proposed in [Helbing and Molnar 1995] to simulate the dynamics of crowds, which provides us an agent-to-agent discrete system that our disease-immunity model is embedded on.

2.2 Disease Simulation

Numerous mathematical studies regarding disease spreading have been conducted during the last few decades. Below, we only review those prior models that have been used to model the spread of COVID-19, since our focus is on the current pandemic, and models for other diseases more or less follow the same methodology.

The well-known SIR (susceptible-infectious–removed, or recovered) model has been extensively analyzed [Hethcote 2000] and extended to finer compartments (see [Pastor-Satorras et al. 2015] for an overview) that mimic the described course of disease spread, deaths, and immunity buildup. SIR-based models have been abundantly applied to locally analyze COVID-19 outbreak dynamics in various countries [Pedersen and Meneghini 2020; Peirlinck et al. 2020]. However, models to predict the temporal and spatial spreading of the virus have so far been rather limited.

Another category of population disease spreading models simulate the state of individual people, known as *agents*, over a number of discrete time steps. Recent studies of agent-based disease simulations for COVID-19 can be found in [Gomez et al. 2020; Kerr et al. 2021; Shamil et al. 2021]. While agent-based models [Eubank et al. 2004] successfully cover the "high-resolution end" at the level of individual people and their movement, the "zoomed-out view" on a state- or county-level is understudied territory, even though statistics at this scale are the ones that influence political decisions the most. A variant of the SIR model has previously been coupled to a reaction-diffusion model [Yamazaki and Wang 2017] to mathematically study disease spreading dynamics with partial differential equations (PDEs). Colizza et al. [2006] have focused on the importance of the air travel network as a basis for global diffusion at a pandemic outbreak. Following this strategy, an air travel network model coupled to an SIR-based model was developed in [Linka et al. 2020; Peirlinck et al. 2020] to understand the *spatial spreading* of the virus. The global epidemic and mobility (GLEAM) model [Balcan et al. 2009] includes air travel as the major source of wide-range disease spreading; it also models more localized commuting patterns that correspond well to traffic data in Germany, among other countries. The model has explained a great deal of COVID-19 spreading at the national scale [Chinazzi et al. 2020].

Models coupling crowd motion and contagion dynamics are far less investigated. We refer to Ref. [Kim and Quaini 2020] for a recent investigation coupling a crowd motion model with a contagion model in a one-dimensional situation. [Abdul Salam et al. 2021] proposed a PDE-based model to investigate the disease contagion within a moving crowd, where an SIR-based model is used for the disease contagion and a continuum approach is used for crowd simulation. To the best of our knowledge, *none* of the prior works have studied the specific disease contagion at the agent-to-agent scale within moving crowds. It is worth nothing that studies regarding disease spreading at the *agent-to-agent* scale are vital, as they use the most basic element of disease transmissions, and they are more intuitive than those at larger scales. Large-scale simulations need to satisfy statistical requirements, such as the size of the overall population in an SIR-based model and the condition of continuity in fluid-like crowd simulations, to guarantee their reliability.

2.3 Our Approach vs. State-of-the-Art

As described above, state-of-the-art disease models primarily fall into two categories: a) SIR-based models, and b) agent-based models. SIR-based models use a set of ordinary differential equations and mainly focus on the evolution of the overall number of susceptible (S), infected (I), and recovered/removed (R) people in a population. They do not provide detailed information regarding individual

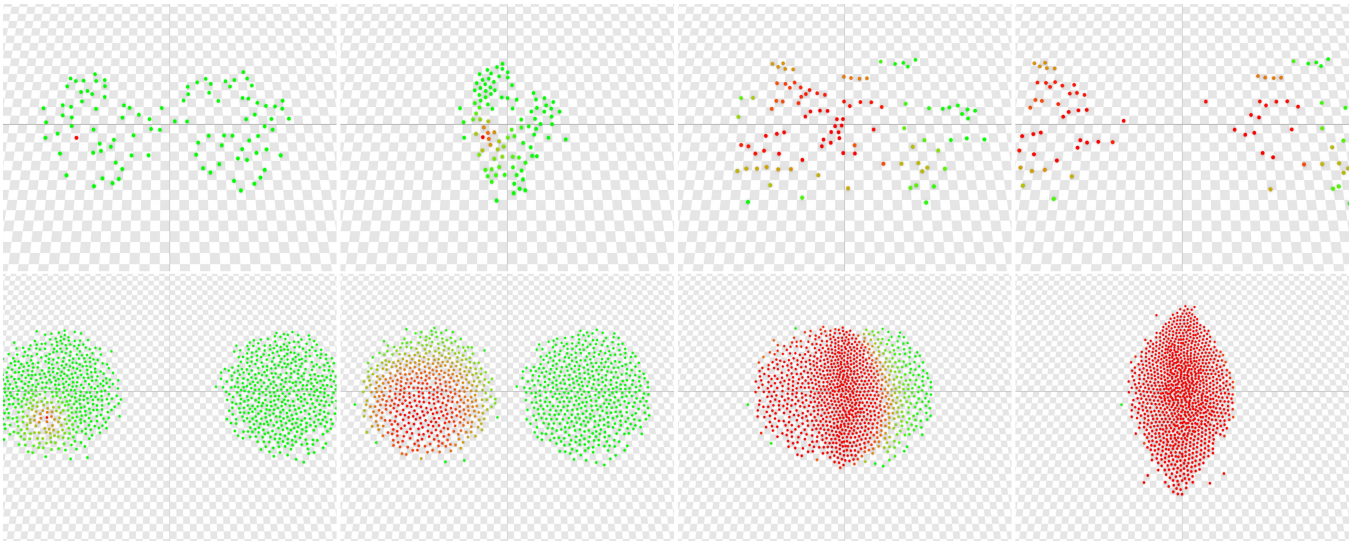

Figure 3: Disease spreading in crowds without protection in sparse (top) and dense (bottom) settings. Unlike classical SIR-based simulations, our model provides detailed disease propagation in space and illustrates that being in a dense gathering results in a high risk of infection. The infectivity β is visualized with colors from green ($\beta = 0$) to red ($\beta \geq 0.5$) for increasing values.

spatial distributions of S, I, and R people. This is also reflected in their mathematical models which have no spatial derivatives.

In contrast to SIR-based models, agent-based disease models can show the distribution of S, I, and R people *geometrically* [Kergaßner et al. 2020; Skvortsov et al. 2007]. Classical agent-based disease models rely heavily upon *contact tracing*, which is the statistical process of identifying people who came within close proximity of infected people. To obtain contact times that communicate the infection, actual census [Hinch et al. 2021; Skvortsov et al. 2007], population-mobility data [Fazio et al. 2021], and social networks [Ehrhardt et al. 2019; Wolfram 2020] have been used. Based on the computed contact times, the infection is passed from one agent to another agent in close proximity at a fixed "contact rate". Likewise, an individual recovers from the infection based on a "recovery rate". Such a disease transmission process that depends purely on contact times ignores the interaction between immunity, infectivity, and vaccination, which are all vital to disease spreading. While such simplified disease transmission processes may yield reasonable results for a large population, they will lose accuracy for smaller crowds, such as a parade, where the number of contacts in any small-scale event is not significantly high and the infection of each individual is mainly determined by the disease-immunity interaction.

Our model focuses on the disease spreading within a moving crowd on a discrete level, and thus, belongs to the category of agent-based models. However, unlike existing agent-based disease models, our focus is on the disease spreading in small-scale events, such as a parade, concert, and school, with the aim of providing detailed information about, for example, *who* is infected, *where* is this infected person, and *how long* will this specific individual take to recover under vaccination? Such low-level information cannot be achieved with existing agent-based models or SIR-based models.

3 GOVERNING EQUATIONS

We now present the governing equations of motion underlying our physics-based model for crowd simulation and disease spreading.

3.1 Crowd Simulation using Social Force

Our model for crowd simulation uses the concept of the *social force* [Helbing and Molnar 1995], which reproduces most empirical observations in a simple and natural way. Reliable simulation of pedestrian crowds does not require knowledge of whether a certain pedestrian (say) turns to the right at the next intersection. It is sufficient to have a good estimate of the *percentage of pedestrians* that turn to the right. This can either be empirically measured or estimated by means of route choice models [Hoogendoorn and HL Bovy 2003; Kosov et al. 2016]. In some sense, the uncertainty about the individual behaviors of people is averaged out at the macroscopic level. Nevertheless, we use the more flexible microscopic simulation approach based on the concept of the social force. According to this model, the temporal change of the location $\mathbf{r}_i(t)$ and the velocity $\mathbf{v}_i(t)$ of pedestrian i obeys the following equation:

$$\frac{d\mathbf{r}_i(t)}{dt} = \mathbf{v}_i(t), \quad \frac{d\mathbf{v}_i(t)}{dt} = \mathbf{f}_i(t) \tag{1}$$

where $\mathbf{f}_i(t)$ denotes the total force experienced by pedestrian i. Suppose each individual i is trying to move in a desired direction $\mathbf{e}_i^0$ with a desired speed v_i^0, so that the desired velocity can be defined as $\mathbf{v}_i^0 = v_i^0 \mathbf{e}_i^0$. The actual velocity $\mathbf{v}_i$ is adapted to the desired one within a certain relaxation time τ_i. The systematic part $\mathbf{f}_i(t)$ of the governing equation of motion for pedestrian i is given as follows:

$$\mathbf{f}_i(t) = \frac{1}{\tau_i}\left[\mathbf{v}_i^0(t) - \mathbf{v}_i(t)\right] + \sum_{j \in \Omega_i} \mathbf{f}_{ij}(t) \tag{2}$$

where the term $\frac{1}{\tau_i}\left[\mathbf{v}_i^0(t) - \mathbf{v}_i(t)\right]$ corresponds to the navigation term (which steers pedestrians towards their destination), and $\mathbf{f}_{ij}$ represents the interaction force between agent i and agent j. The specific equation for $\mathbf{f}_{ij}$ is given as follows:

$$\mathbf{f}_{ij} = Ae^{-b_{ij}/B} \cdot \frac{\|\mathbf{r}_{ij}\| + \|\mathbf{r}_{ij} - \mathbf{y}_{ji}\|}{2b_{ij}} \left(\frac{\mathbf{r}_{ij}}{\|\mathbf{r}_{ij}\|} + \frac{\mathbf{r}_{ij} - \mathbf{y}_{ji}}{\|\mathbf{r}_{ij} - \mathbf{y}_{ji}\|} \right) \tag{3}$$

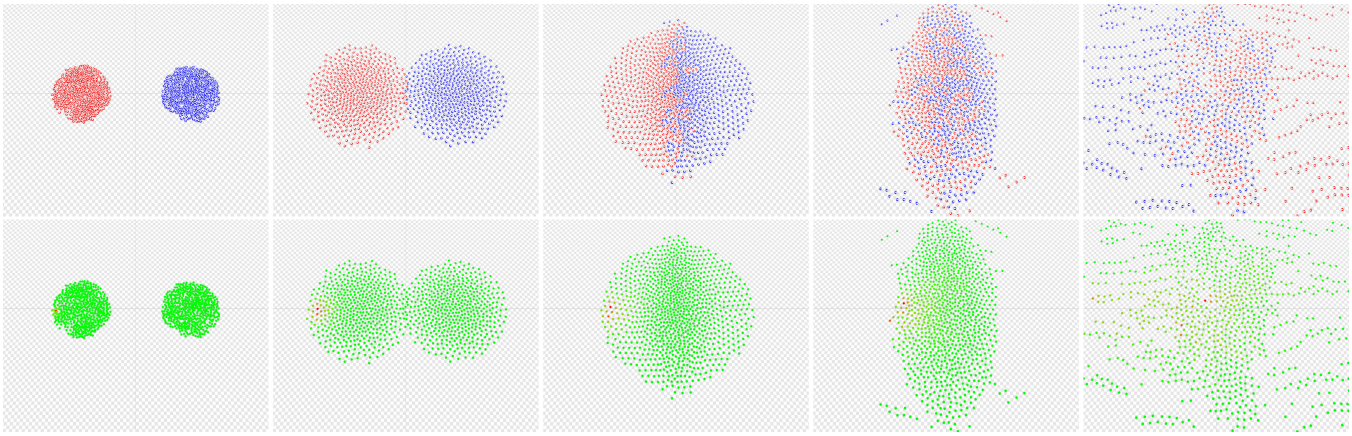

Figure 4: Our model successfully captures the expansion of dense crowds due to social distancing restrictions (top). Consequently, as the distance between two agents increases, only a few agents are infected, as illustrated by the spatial distribution of the disease (bottom). The infectivity β is visualized with colors from green ($\beta = 0$) to red ($\beta \geq 0.5$) for increasing values.

where A reflects the interaction strength of the force, B corresponds to the interaction range, $\mathbf{r}_{ij} = \mathbf{r}_i - \mathbf{r}_j$, $\mathbf{y}_{ji} = (\mathbf{v}_j - \mathbf{v}_i)\,\Delta t$, and $b_{ij} = 0.5\sqrt{(\|\mathbf{r}_{ij}\| + \|\mathbf{r}_{ij} - \mathbf{y}_{ji}\|)^2 - \|\mathbf{y}_{ji}\|}$.

3.2 Disease Contagion Model

In contrast to prior SIR-based models and the continuous diffusion model [Kuniya 2020], we develop an agent-to-agent disease contagion model that focuses on the coupling between infection and immunity at the agent scale. By doing this, our model allows us to investigate detailed disease spreading within crowds with a limited number of agents, in which the spatially continuous diffusion-based disease model is not applicable as it requires spatial continuity.

3.2.1 Discrete diffusion model. We define disease, or infectivity, as a diffusive quantity β_i for agent i in a population of agents. There is a disease spreading bond between any close-enough pair of agents i and j. The two agents have different infectivities β_i and β_j, respectively. Without loss of generality, assume that $\beta_j > \beta_i$. Based on the principles of diffusion [Carslaw 1906], the diffusive quantities (e.g., atoms, ions, molecules, energy) will automatically move from a region of higher concentration to a region of lower concentration. We utilize this concept to define a visual diffusive bond between agents i and j. We assume that the diffusion within the bond $i \leftrightarrow j$ follows Fourier's law, such that the infectivity flowing between agents i and j over an area s in t seconds equals:

$$k_{ij}\frac{(\beta_j - \beta_i)\cdot s \cdot t}{d_{ij}} \tag{4}$$

where $d_{ij} = \|\mathbf{r}_j - \mathbf{r}_i\|$ is the distance between agents i and j, k_{ij} is the propagation coefficient representing the amount of infectivity β that is transported from agent j to i under the influence of the difference $(\beta_j - \beta_i)$. We define $\beta^a_{i\leftrightarrow j}$ as the average infectivity in the bond $i \leftrightarrow j$. The rate at which the infective bond gains volumnic infectivity is defined as:

$$s \cdot d_{ij} \cdot \frac{D\beta^a_{i\leftrightarrow j}}{Dt} \tag{5}$$

where D/Dt represents the *material derivative*. Based on the conservation of energy [Meltzer 2004], the infective equation for per unit area and per unit time is given as follows:

$$s \cdot d_{ij} \cdot \frac{D\beta^a_{i\leftrightarrow j}}{Dt} = k_{ij}\frac{(\beta_j - \beta_i)\cdot s}{d_{ij}} \tag{6}$$

The governing equation for disease propagation within the bond between agents i and j can be written as follows:

$$\frac{D\beta^a_{i\leftrightarrow j}}{Dt} = k_{ij}\frac{\beta_j - \beta_i}{d^2_{ij}} \tag{7}$$

We consider the average of all disease bonds within a limited contagious range of agent i, denoted as Ω_i. Thus, our agent-based disease contagion model is given as follows:

$$\frac{D\beta_i}{Dt} = \frac{1}{n_i}\sum_{j\in\Omega_i}\frac{D\beta^a_{i\leftrightarrow j}}{Dt}W_{ij} = \frac{1}{n_i}\sum_{j\in\Omega_i}k_{ij}\frac{\beta_j - \beta_i}{d^2_{ij}}W_{ij} \tag{8}$$

where W_{ij} represents the weight value of agent j in the neighboring domain of agent i, and $n_i = \sum_{j\in\Omega_i} W_{ij}$, which normalizes the weighting process. Given that the possibility of getting infected decays if the distance from the infected source becomes large, we define k_{ij} as follows:

$$k_{ij} = e^{-\frac{d_{ij}}{R_s}} \tag{9}$$

where R_s is the infectivity range, which is equivalent to the social force interaction range B in equation (3). Based on equation (9), we simulate how practicing social distancing helps to block the virus spread by strengthening the social force's interaction strength A (see equation (3)), and by increasing the distance limit beyond which the social force is not computed between individuals.

3.3 Contagion-immunity Coupling System

Inspired by [Macal 2010; Xiao and Chen 2001] that couple predator-prey model in the SIR-based models and the classical agent-based disease models, we further extend our agent-based disease contagion model in equation (8) to account for the interaction between agent-based immunity and contagion by using the *predator-prey* model [Berryman 1992; Pang and Wang 2003] with diffusion.

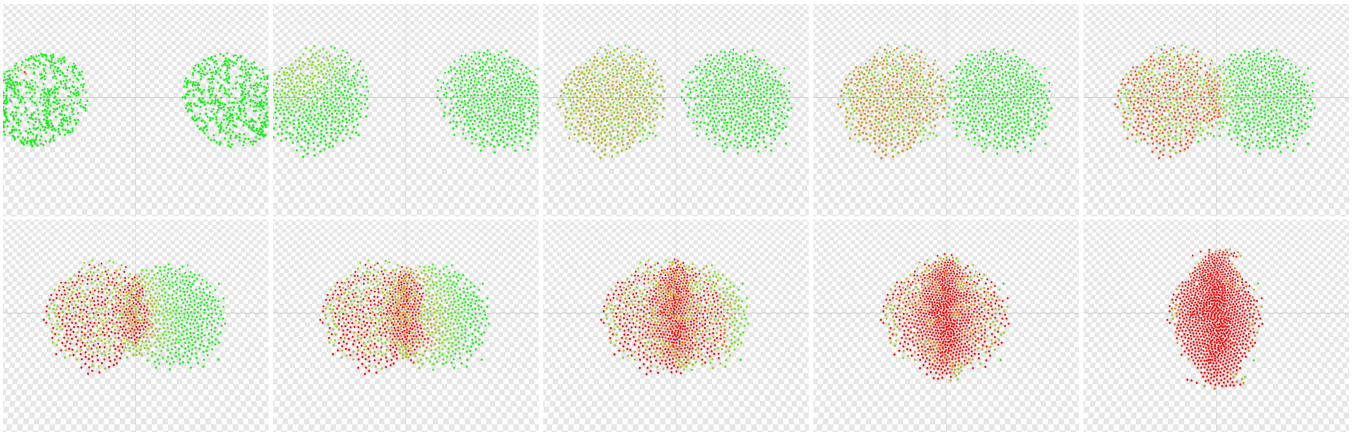

Figure 5: Our model captures realistic disease-immunity interactions and provides detailed infectivity of each agent. The disease was first prevented by inner immunity (top). However, the highly contagious COVID-19 infects more agents as the number of contacts increase. The infectivity β is visualized with colors from green ($\beta = 0$) to red ($\beta \geq 0.5$) for increasing values.

3.3.1 Contagion. On one hand, the contagion is affected by neighboring agents as shown in equation (8). On the other hand, the inner immune system plays a role in defeating the virus and balancing the contagion. Given the above, our model for contagion at agent i is given by:

$$\frac{D\beta_i}{Dt} = \frac{1}{n_i} \sum_{j \in \Omega_i} k_{ij} \frac{\beta_j - \beta_i}{d_{ij}^2} W_{ij} + \beta_i(\sigma - \beta_i) - \frac{a\beta_i^2 \alpha_i}{1 + \beta_i^2} \tag{10}$$

where β_i and α_i represent the contagion and immunity of agent i, respectively. The term $\beta_i(\sigma - \beta_i)$ describes the *prey* in the absence of predators and harvesting. The term $a\beta_i^2\alpha_i/(1 + \beta_i^2)$ is termed a Holling-III response function [Holling 1959] describing the inhibition due to immunity α_i. a and σ are user-defined parameters.

3.3.2 Immunity equation. The mechanism of the immune system is very complex when the body is under the attack of a virus. The virus first stimulates the immune system to fight, and if the agent has a sufficiently strong immune system, it wins the fight. Otherwise, the agent is highly susceptible to getting infected and becomes a source of infection. To describe the immunity of agent i, the inhibition and enhancement of immunity due to inherent reasons (e.g., current health condition) and due to the contagion are considered in our model. Moreover, given that the immune system is also affected by getting a *vaccine*, we utilize a hyperbolic tangent term to describe the re-boosting of the immune system after getting vaccinated. The specific model of immunity is given as follows:

$$\frac{D\alpha_i}{Dt} = \frac{\gamma_i \beta_i^2}{1 + \beta_i^2} \alpha_i + \mu\alpha_i + \sum_{j=0}^{2} \xi \tanh(t - t_\xi) \tag{11}$$

where the term $\frac{\gamma_i\beta_i^2}{1+\beta_i^2}\alpha_i$ represents the influences of the contagion on the immunity, and γ_i is a user-defined parameter. When $\gamma = 1$, the virus stimulates the immune system, while for $\gamma < 0$, the virus inhibits the immune system. In our simulations, we chose $\gamma = -0.5$ as the COVID-19 virus can readily break the human immune system and cause severe illness. μ_j represents the inherent strength of the immune system. If the agent has a healthy lifestyle, μ is set to be 0.1, while if the agent has an unhealthy lifestyle, μ is set to be -0.1. The term $\sum_{j=1}^{v} \xi \tanh(t - t_\xi)$ describes the boost to the immune system due to the vaccine. In our model, we assume a single dose of vaccine is fully effective, and the strength of the immune system will be re-boosted when more doses of the vaccine are taken. ξ represents the strength of a vaccine shot.

4 DISCRETIZATION

Although implicit schemes have been acknowledged to be more efficient than explicit schemes and allow for larger time steps in the simulations, the time step Δt is required to be small to accurately capture the contact between agents. We use the simple forward Euler time integration to discretize the coupling between the equation of crowd motion (1), the infectivity equation (10), and the immunity equation (11), and update $\mathbf{r}_i$, $\mathbf{v}_i$, β_i and α_i at t_{n+1} as follows:

$$\begin{aligned}
\beta_i^{n+1} &= \beta_i^n + \frac{\Delta t}{n_i^n} \sum_{j \in \Omega_i} k_{ij}^n \frac{\beta_j^n - \beta_i^n}{(d_{ij}^2)^n} W_{ij}^n + \beta_i^n(s - \beta_i^n) - \left(\frac{a\beta_i^2\alpha_i}{1 + \beta_i^2}\right)^n \\
\alpha_i^{n+1} &= \alpha_i^n + \frac{\gamma_i \Delta t (\beta_i^n)^2}{1 + (\beta_i^n)^2} \alpha_i^n + \mu \Delta t \alpha_i^n + \Delta t \sum_{\xi=0}^{2} \xi \tanh(t^n - t_\xi^n) \\
\mathbf{v}_i^{n+1} &= \frac{1}{\tau_i}\left(\mathbf{v}_i^0 - \mathbf{v}_i^n\right) + \\
&\sum_{j \in \Omega_i} \left[A e^{-\frac{b_{ij}^n}{B}} \cdot \frac{\|\mathbf{r}_{ij}^n\| + \|\mathbf{r}_{ij}^n - \mathbf{y}_{ji}^n\|}{2b_{ij}^n} \left(\frac{\mathbf{r}_{ij}^n}{\|\mathbf{r}_{ij}^n\|} + \frac{\mathbf{r}_{ij}^n - \mathbf{y}_{ji}^n}{\|\mathbf{r}_{ij}^n - \mathbf{y}_{ji}^n\|} \right) \right] \\
\mathbf{r}_i^{n+1} &= \mathbf{r}_i^n + \Delta t \mathbf{v}_i^{n+1}
\end{aligned} \tag{12}$$

where the superscript n denotes variables at time t^n; t_ξ^n represents the time instant when the ξ-th dose of the vaccine is taken.

5 RESULTS

Accompanying this article, we open-source our code for running all our examples with the proposed computational framework for simulating contagion-immunity interactions within moving crowds. All our examples are run on a 1.30 GHz to 1.50 GHz, Intel(R) Core(TM)

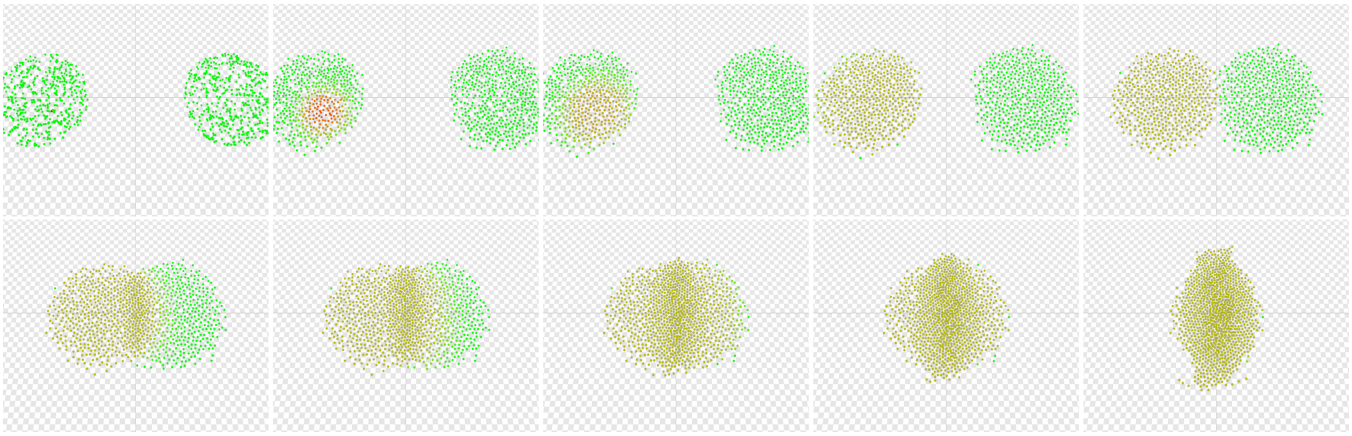

Figure 6: Our model shows that vaccination can effectively decay the disease spread and suppress the infectivity of the entire crowd to a very low value. The infectivity β is visualized with colors from green ($\beta = 0$) to red ($\beta \geq 0.02$) for increasing values.

i7-1065G7 CPU with 16GB RAM. For all cases, we set the time step $\Delta t = 0.01$, interaction range $B = 1.0$, relaxation time $\tau = 1.0$, desired speed $v_i^0 = 1.0$, infectious range $R_s = 1.0$, user-defined parameter $\sigma = 1.0$ in equation (10), contagion-immunity coupling parameter $\gamma = -0.5$, and vaccine delay $t_\xi = 0$. Table 1 summarizes the specific parameters that we changed across our simulations.

Table 1: Parameters that vary across simulations: n: number of pedestrians, A: social force interaction strength, r: social force radius, a: immunity strength, and ξ: vaccine factor.

	n	A	r	a	ξ
Unprotected Sparse (Figs. 2 and 3 top)	0.1K	5.0	1.0	0.0	0.0
Unprotected Dense (Figs. 2 and 3 bottom)	1K	5.0	1.0	0.0	0.0
Social Distancing Dense (Fig.4)	1K	10	3.0	0.0	0.0
Immunity Dense (Fig.5)	1K	5.0	1.0	100	0.0
Vaccination Dense (Fig.6)	1K	5.0	1.0	100	0.5

5.1 Crowd Simulations

We experimented with two groups of agents walking in horizontally opposite directions (see Figure 2). The agents in each group are positioned in a sparse particle distribution with an initial separation distance. To avoid collisions, we consider a relatively large influence range Ω_i (long range collision) in equation (8). In this scenario, the agents organize themselves into narrow lanes, and pass each other (see Figure 2(top)). Next, we simulate a dense passing scenario with 1000 agents, which are split into two agent groups. In the dense setting, the two agent groups do not easily pass each other, and some bottleneck groups are formed as shown in Figure 7. Eventually, the agents pass, avoiding unrealistic collisions. Our simulations demonstrate interesting group interactions, such as the formation of lanes and subgroups with minimal interfaces, and qualitatively match with the simulations from position-based methods [Weiss et al. 2019] (see here [2] for a video of the position-based crowd simulation), validating our crowd simulations.

[2] https://www.youtube.com/watch?v=iC8KHkoZR8k&ab_channel=ComputersandGraphicsJournal

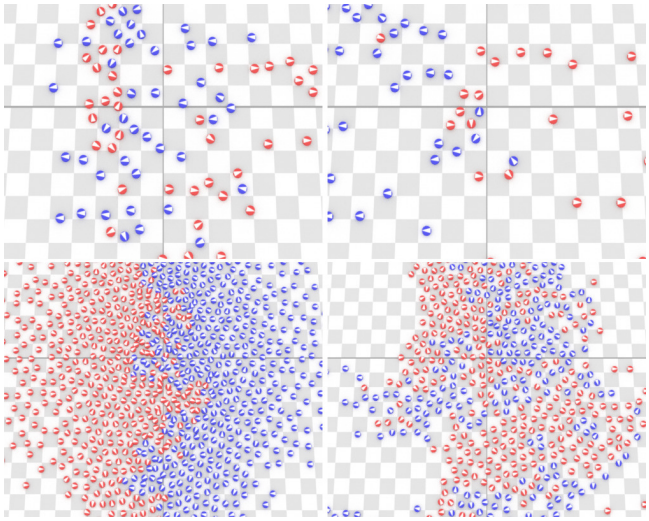

Figure 7: A closer view of group interactions in both sparse (top) and dense passing (bottom) examples from Figure 2.

5.2 Disease Contagion in Moving Crowds

5.2.1 Unprotected. We simulated the disease contagion in the moving crowds whose group interactions are described in Section 5.1. We first show the disease contagion in crowds without any protections such as social distancing and immunity. As shown in Figure 3, initially only one agent is infected. As agent-to-agent contacts increase, more agents become infected. In the case of a sparse distribution, since the overall distance between any two agents is farther than in the dense distribution case, the disease propagates at a significantly slower pace than that in the dense crowd.

5.2.2 Social Distancing. Our model can be used to investigate the effect of social distancing. We strengthen the social force in equation (2) by increasing variable A and increase the social force radius r (see Table 1). The social force is only calculated between agents whose distances are less than the social force radius. We simulated disease spreading in dense crowds, as shown in Figure 4. Due to the increased social force, the dense crowds expand before and while walking in opposite directions. Since all the agents obey the

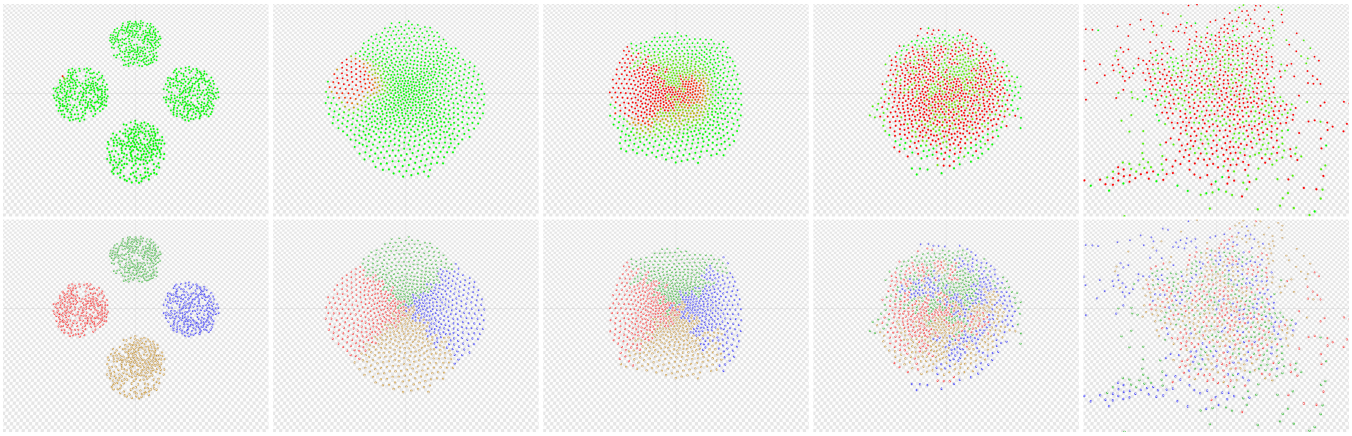

Figure 8: Simulation of disease spreading in four groups (bottom) with different health interventions (Red: Unprotected, Green: Immunity only, Blue: Unprotected, and Brown: Immunity and Vaccinated) mixing from different directions. We show the infectivity evolution (top) during mixing. The infectivity β is visualized with colors from green ($\beta = 0$) to red ($\beta = 1$).

social distancing restriction, we observe that the disease spreads at a slower pace and only within a very small range of agents near the infected source.

5.2.3 Immunity. Next, we consider the effect of immunity, as shown in equation (11). This case is without vaccinations, so $\xi = 0$. As all the agents are protected by their inner immunity, the degree of the illness of infected agents relies heavily upon the "fight" between the immunity and the disease. Our model demonstrates that immunity can protect agents from the disease to a certain degree. However, given the high contagiousness of COVID-19, a majority of the population in the groups are eventually infected. This agrees with the CDC's published conclusions regarding the contagion of COVID-19 [3]. As shown in Figure 5, we initially consider only one infected agent, as the inner immunity starts to play a role, the virus is suppressed to a certain extent (see Figure 5(top)). However, as time goes by, the virus in each agent gradually grows and leads more agents to become infected. Our model captures this realistic interaction between infectivity and immunity, showcasing that COVID-19 can break human immunity.

5.2.4 Vaccination. Our model can also be used to simulate the disease propagation under the influence of a vaccine. The vaccine term in equation (11) boosts the inner immunity of each agent. As the immunity is strengthened, it significantly prevents the infection and decreases the number of infected people in the groups. In Figure 6, we simulated the same scenario shown in Figure 5, but with the strong protection of the vaccine. As shown in Figure 6, vaccines can slow the spread of COVID-19, accelerate healing from COVID-19, and overcome the ongoing threat of the pandemic.

5.2.5 Multiple groups interaction. We also investigated the disease propagation within moving crowds under different health interventions. Four groups of agents (see Figure 8) are assigned different walking directions, as well as different health intervention approaches, including unprotected, immunity, and vaccination. As shown in Figure 8, vaccinated agents slow down the spread of COVID-19 within the overall groups.

[3] https://www.cdc.gov/coronavirus/2019-ncov/hcp/ways-operate-effectively.html

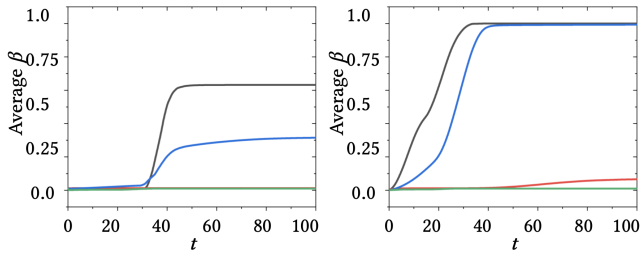

Figure 9: Infectivity Evolution. Black: Unprotected, Red: Social Distancing, Blue: Immunity, and Green: Vaccination. Our model implies that infectivity in a sparse crowd (left) is significantly slower and smaller than in a dense crowd (right). Our model also shows that social distancing and vaccination are the two most promising ways of avoiding disease spreading in crowds. Vaccination appears to be the best protection against a highly contagious disease.

5.3 Quantitative Evaluations

5.3.1 Infectivity. We first quantitatively compare the evolution of the average infectivity (β) showcasing how different public health interventions may affect the outcome of the pandemic. As shown in Figure 9, we found that disease spreading in sparse crowds is significantly slower than in dense crowds, and the amount of average infectivity is significantly less in sparse crowds than in dense crowds. Our model also demonstrates that immunity has limited effects in alleviating the speed of disease spread and decreasing the average infectivity in sparse crowds. However, immunity may lose its strength, particularly in dense crowds. Comparing different scenarios, we observed that for sparse crowds, the policy of social distancing and vaccination have a similar performance in preventing the overall infectivity, while vaccination is the best way to lower the average infectivity in dense crowds.

5.3.2 Comparison with SIS. Next, we show the comparison with the famous SIS (susceptible-infectious-susceptible) model [Gray et al. 2011; Otunuga 2021], which is a variant of SIR model. The SIS model has been used to describe a disease that does not confer any long-lasting immunity. Such infections do not give immunity upon recovery from infection, and individuals become susceptible

again. In the long term, all individuals will become infected in the SIS model. We treat agents with $\beta \leq 0.5$ as infected people and demonstrate that the changing trend of the total number of infected people agrees with the SIS model in the case of *unprotected dense crowds* (see Figure 10(left)), while crowds with a sparse distribution and/or proper health interventions delay or eliminate the trend of increasing infections in the population.

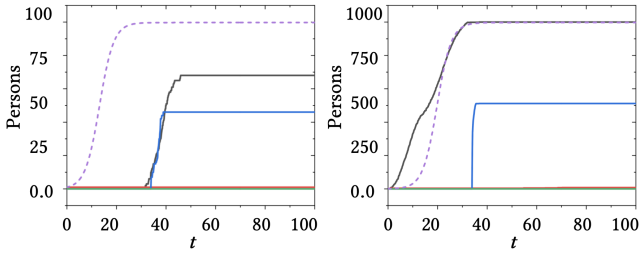

Figure 10: Infectivity Evolution. Left: Sparse crowd. Right: Dense crowd. Purple dot line: SIS model, Black: Unprotected, Red: Social Distancing, Blue: Immunity, and Green: Vaccination. The number of infected people in the dense unprotected crowd in our model agrees with the SIS model, while the other cases from our model provide more reasonable trends of change in the infected population.

Figure 11: Snapshot from our interactive framework for simulating disease spreading in moving crowds. Typing "D" switches the display mode between showing particle groups (top left) or particle disease status (top right), while clicking any particle can mark that particle as fully infected, turning its color to red ($\beta = 1$, see bottom left). Typing "S" advances the simulation by ten time steps, showing the details of the disease spread (bottom right).

5.4 Interactive Simulations

To demonstrate the power and flexibility of our model, we developed an interactive version of our framework, where a user can pause the simulation and change various attributes of the simulated people. As shown in Figure 11, clicking on a person immediately labels that person as being fully infected (i.e., $\beta = 1$). As time goes by, the disease from this infected person first transmits to neighboring agents, possibly spreading the disease to the entire group. Our interactive application supports infecting multiple agents at any time, allowing the user to simulate different scenarios of disease spread. We release our code for the interactive simulations so that a user can integrate more related modules in our framework.

6 DISCUSSIONS AND CONCLUSION

We proposed an agent-based contagion-immunity formulation that provides detailed disease spreading of COVID-19 and immune reaction within moving crowds. In contrast to most prior work based on large populations and SIR-based formulations, our model focuses on systems with a limited population, which cannot be treated with continuum formulations. We demonstrated that our methods capture realistic disease spreading in both sparse and dense crowds under different health interventions, such as social distancing, immunity, and vaccination. We found out that the disease spread in sparse crowds is significantly slower than in dense crowds, and that vaccination is the best way to lower infectivity.

Our model has generated a large number of compelling examples, and agrees with the SIS model, but there remains much work to be done. Parameters to adjust infection range, interaction range, and the like were tuned by hand, and it would be interesting to calibrate them to measured models. While we did not experience a need for excessively small time steps during simulations, it would be interesting to incorporate multi-rate time integration schemes into our framework to support different time steps on different disease spreading scenarios. Besides, though the extra diffusion term in our predator-prey model (see equation (10)) smooths the numerical results, which allows us to use a forward Euler scheme for the predator-prey model, it would also be interesting to use symplectic Euler schemes to solve the contagion-immunity coupling system. Another limitation of our work stems from the crowd simulations. It would be interesting to develop the disease spreading model based on position-based crowd simulations [Weiss et al. 2019].

ACKNOWLEDGMENTS

We thank the anonymous reviewers for their valuable feedback which greatly helped in improving the exposition. This research was supported in part by the Rutgers University start-up grant and the National Science Foundation under award CCF-2110861. Any opinions, findings, and conclusions or recommendations expressed in this material are those of the authors and do not necessarily reflect the views of the National Science Foundation.

REFERENCES

Parveena Shamim Abdul Salam, Wolfgang Bock, Axel Klar, and Sudarshan Tiwari. 2021. Disease contagion models coupled to crowd motion and mesh-free simulation. *Mathematical Models and Methods in Applied Sciences* (2021), 1–19.

Duygu Balcan, Vittoria Colizza, Bruno Gonçalves, Hao Hu, José J Ramasco, and Alessandro Vespignani. 2009. Multiscale mobility networks and the spatial spreading of

infectious diseases. *Proceedings of the National Academy of Sciences* 106, 51 (2009), 21484–21489.

Nicola Bellomo and Christian Dogbe. 2011. On the modeling of traffic and crowds: A survey of models, speculations, and perspectives. *SIAM review* 53, 3 (2011), 409–463.

Alan A Berryman. 1992. The orgins and evolution of predator-prey theory. *Ecology* 73, 5 (1992), 1530–1535.

Ling Bian. 2004. A conceptual framework for an individual-based spatially explicit epidemiological model. *Environment and Planning B: Planning and Design* 31, 3 (2004), 381–395.

Wolfgang Bock, Barbara Adamik, Marek Bawiec, Viktor Bezborodov, Marcin Bodych, Jan Pablo Burgard, Thomas Goetz, Tyll Krueger, Agata Migalska, Barbara Pabjan, et al. 2020. Mitigation and herd immunity strategy for COVID-19 is likely to fail. *medRxiv* (2020).

Horatio Scott Carslaw. 1906. *Introduction to the Mathematical Theory of the Conduction of Heat in Solids*. Dover.

Alice Cartaud, François Quesque, and Yann Coello. 2020. Wearing a face mask against Covid-19 results in a reduction of social distancing. *Plos one* 15, 12 (2020), e0243023.

Joydev Chattopadhyay and Ovide Arino. 1999. A predator-prey model with disease in the prey. *Nonlinear analysis* 36 (1999), 747–766.

Matteo Chinazzi, Jessica T Davis, Marco Ajelli, Corrado Gioannini, Maria Litvinova, Stefano Merler, Ana Pastore y Piontti, Kunpeng Mu, Luca Rossi, Kaiyuan Sun, et al. 2020. The effect of travel restrictions on the spread of the 2019 novel coronavirus (COVID-19) outbreak. *Science* 368, 6489 (2020), 395–400.

Rajiv Chowdhury, Kevin Heng, Md Shajedur Rahman Shawon, Gabriel Goh, Daisy Okonofua, Carolina Ochoa-Rosales, Valentina Gonzalez-Jaramillo, Abbas Bhuiya, Daniel Reidpath, Shamini Prathapan, et al. 2020. Dynamic interventions to control COVID-19 pandemic: a multivariate prediction modelling study comparing 16 worldwide countries. *European journal of epidemiology* 35, 5 (2020), 389–399.

Vittoria Colizza, Alain Barrat, Marc Barthélemy, and Alessandro Vespignani. 2006. The role of the airline transportation network in the prediction and predictability of global epidemics. *Proceedings of the National Academy of Sciences* 103, 7 (2006), 2015–2020.

Alessandro Comunian, Romina Gaburro, and Mauro Giudici. 2020. Inversion of a SIR-based model: a critical analysis about the application to COVID-19 epidemic. *Physica D: Nonlinear Phenomena* 413 (2020), 132674.

J Alberto Conejero, Enrique Hernández-Orallo, Pietro Manzoni, and Marina Murillo-Arcila. 2019. A SIR-based model for contact-based messaging applications supported by permanent infrastructure. *Discrete & Continuous Dynamical Systems-S* 12, 4&5 (2019), 735.

Russell Connell, Peter Dawson, and Alex Skvortsov. 2009. *Comparison of an agent-based model of disease propagation with the generalised SIR epidemic model*. Technical Report. DEFENCE SCIENCE AND TECHNOLOGY ORGANISATION VICTORIA (AUSTRALIA) AIR ….

Bruno Di Stefano, Henryk Fuks, and Anna T Lawniczak. 2000. Object-oriented implementation of CA/LGCA modelling applied to the spread of epidemics. In *2000 Canadian Conference on Electrical and Computer Engineering. Conference Proceedings. Navigating to a New Era (Cat. No. 00TH8492)*, Vol. 1. IEEE, 26–31.

T. B. Dutra, R. Marques, J.B. Cavalcante-Neto, C. A. Vidal, and J. Pettré. 2017. Gradient-based steering for vision-based crowd simulation algorithms. *Computer Graphics Forum* 36, 2 (2017), 337–348.

Matthias Ehrhardt, Ján Gašper, and Soňa Kilianová. 2019. SIR-based mathematical modeling of infectious diseases with vaccination and waning immunity. *Journal of Computational Science* 37 (2019), 101027.

Joshua M Epstein, Derek AT Cummings, Shubha Chakravarty, Ramesh M Singha, and Donald S Burke. 2012. *Toward a containment strategy for smallpox bioterror: an individual-based computational approach*. Princeton University Press.

Raghavender Etikyala, Simone Göttlich, Axel Klar, and Sudarshan Tiwari. 2014. Particle methods for pedestrian flow models: from microscopic to nonlocal continuum models. *Mathematical Models and Methods in Applied Sciences* 24, 12 (2014), 2503–2523.

Stephen Eubank, Hasan Guclu, VS Anil Kumar, Madhav V Marathe, Aravind Srinivasan, Zoltan Toroczkai, and Nan Wang. 2004. Modelling disease outbreaks in realistic urban social networks. *Nature* 429, 6988 (2004), 180–184.

Martina Fazio, Alessandro Pluchino, Giuseppe Inturri, Michela Le Pira, Nadia Giuffrida, and Matteo Ignaccolo. 2021. Exploring the impact of mobility restrictions on the COVID-19 spreading through an agent-based approach. *arXiv preprint arXiv:2102.08226* (2021).

Mauro Giudici, Alessandro Comunian, and Romina Gaburro. 2020. Inversion of a SIR-based model: A critical analysis about the application to COVID-19 epidemic. *arXiv preprint arXiv:2004.07738* (2020).

Jonatan Gomez, Jeisson Prieto, Elizabeth Leon, and Arles Rodriguez. 2020. INFEKTA: a general agent-based model for transmission of infectious diseases: studying the COVID-19 propagation in Bogotá-Colombia. *MedRxiv* (2020).

Alison Gray, David Greenhalgh, Liangjian Hu, Xuerong Mao, and Jiafeng Pan. 2011. A stochastic differential equation SIS epidemic model. *SIAM J. Appl. Math.* 71, 3 (2011), 876–902.

Dirk Helbing. 1998. A fluid dynamic model for the movement of pedestrians. *arXiv preprint cond-mat/9805213* (1998).

Dirk Helbing and Peter Molnar. 1995. Social force model for pedestrian dynamics. *Physical review E* 51, 5 (1995), 4282.

Omar Hesham and Gabriel Wainer. 2021. Advanced models for centroidal particle dynamics: short-range collision avoidance in dense crowds. *SIMULATION* (2021), 00375497211003126.

Herbert W Hethcote. 2000. The mathematics of infectious diseases. *SIAM review* 42, 4 (2000), 599–653.

Robert Hinch, William JM Probert, Anel Nurtay, Michelle Kendall, Chris Wymant, Matthew Hall, Katrina Lythgoe, Ana Bulas Cruz, Lele Zhao, Andrea Stewart, et al. 2021. OpenABM-Covid19—An agent-based model for non-pharmaceutical interventions against COVID-19 including contact tracing. *PLoS computational biology* 17, 7 (2021), e1009146.

Crawford S Holling. 1959. The components of predation as revealed by a study of small-mammal predation of the European Pine Sawfly1. *The Canadian Entomologist* 91, 5 (1959), 293–320.

Serge Hoogendoorn and Piet HL Bovy. 2003. Simulation of pedestrian flows by optimal control and differential games. *Optimal control applications and methods* 24, 3 (2003), 153–172.

Hao Jiang, Zhigang Deng, Mingliang Xu, Xiangjun He, Tianlu Mao, and Zhaoqi Wang. 2018. An emotion evolution based model for collective behavior simulation. In *Proceedings of the ACM SIGGRAPH Symposium on Interactive 3D Graphics and Games*. 1–6.

Hao Jiang, Wenbin Xu, Tianlu Mao, Chunpeng Li, Shihong Xia, and Zhaoqi Wang. 2010. Continuum crowd simulation in complex environments. *Computers & Graphics* 34, 5 (2010), 537–544.

Zengxin Kang, Lei Zhang, and Kun Li. 2019. An improved social force model for pedestrian dynamics in shipwrecks. *Appl. Math. Comput.* 348 (2019), 355–362.

Andreas Kergaßner, Christian Burkhardt, Dorothee Lippold, Matthias Kergaßner, Lukas Pflug, Dominik Budday, Paul Steinmann, and Silvia Budday. 2020. Memory-based meso-scale modeling of Covid-19. *Computational mechanics* 66, 5 (2020), 1069–1079.

William Ogilvy Kermack and Anderson G McKendrick. 1927. A contribution to the mathematical theory of epidemics. *Proceedings of the royal society of london. Series A, Containing papers of a mathematical and physical character* 115, 772 (1927), 700–721.

Cliff C Kerr, Robyn M Stuart, Dina Mistry, Romesh G Abeysuriya, Katherine Rosenfeld, Gregory R Hart, Rafael C Nunez, Jamie A Cohen, Prashanth Selvaraj, Brittany Hagedorn, et al. 2021. Covasim: an agent-based model of COVID-19 dynamics and interventions. *MedRxiv* (2021), 2020–05.

Daewa Kim and Annalisa Quaini. 2020. Coupling kinetic theory approaches for pedestrian dynamics and disease contagion in a confined environment. *Mathematical Models and Methods in Applied Sciences* 30, 10 (2020), 1893–1915.

Sujeong Kim, Stephen J Guy, Karl Hillesland, Basim Zafar, Adnan Abdul-Aziz Gutub, and Dinesh Manocha. 2015. Velocity-based modeling of physical interactions in dense crowds. *The Visual Computer* 31, 5 (2015), 541–555.

Hoshang Kolivand, Mohd Shafry Rahim, Mohd Shahrizal Sunar, Ahmad Zakwan Azizul Fata, and Chris Wren. 2021. An integration of enhanced social force and crowd control models for high-density crowd simulation. *Neural Computing and Applications* 33, 11 (2021), 6095–6117.

Mikhail Evgenievich Kosov, Ravil Gabdullaevich Akhmadeev, Vladimir Sergeevich Osipov, Yulia Konstantinovna Kharakoz, and Irina Ivanovna Smotritskaya. 2016. Socio-economic planning of the economy. *Indian Journal of Science and Technology* 9, 36 (2016), 102008.

Toshikazu Kuniya. 2020. On the Relationship Between the Basic Reproduction Number and the Shape of the Spatial Domain. In *Mathematical Modelling and Analysis of Infectious Diseases*. Springer, 37–59.

Kevin Linka, Mathias Peirlinck, Francisco Sahli Costabal, and Ellen Kuhl. 2020. Outbreak dynamics of COVID-19 in Europe and the effect of travel restrictions. *Computer Methods in Biomechanics and Biomedical Engineering* 23, 11 (2020), 710–717.

Charles M Macal. 2010. To agent-based simulation from system dynamics. In *Proceedings of the 2010 Winter Simulation Conference*. IEEE, 371–382.

David E Meltzer. 2004. Investigation of students' reasoning regarding heat, work, and the first law of thermodynamics in an introductory calculus-based general physics course. *American Journal of Physics* 72, 11 (2004), 1432–1446.

Rahul Narain, Abhinav Golas, Sean Curtis, and Ming C Lin. 2009. Aggregate dynamics for dense crowd simulation. In *ACM SIGGRAPH Asia 2009 papers*. 1–8.

Mark EJ Newman. 2002. Spread of epidemic disease on networks. *Physical review E* 66, 1 (2002), 016128.

Olusegun Michael Otunuga. 2021. Time-dependent probability distribution for number of infection in a stochastic SIS model: case study COVID-19. *Chaos, Solitons & Fractals* 147 (2021), 110983.

Peter YH Pang and Mingxin Wang. 2003. Qualitative analysis of a ratio-dependent predator–prey system with diffusion. *Proceedings of the Royal Society of Edinburgh Section A: Mathematics* 133, 4 (2003), 919–942.

Romualdo Pastor-Satorras, Claudio Castellano, Piet Van Mieghem, and Alessandro Vespignani. 2015. Epidemic processes in complex networks. *Reviews of modern physics* 87, 3 (2015), 925.

Morten Gram Pedersen and Matteo Meneghini. 2020. Quantifying undetected COVID-19 cases and effects of containment measures in Italy. *ResearchGate Preprint (online*

21 March 2020) DOI 10 (2020).

Mathias Peirlinck, Kevin Linka, Francisco Sahli Costabal, and Ellen Kuhl. 2020. Outbreak dynamics of COVID-19 in China and the United States. *Biomechanics and modeling in mechanobiology* 19, 6 (2020), 2179–2193.

Nuria Pelechano, Jan M Allbeck, and Norman I Badler. 2008. Virtual crowds: Methods, simulation, and control. *Synthesis lectures on computer graphics and animation* 3, 1 (2008), 1–176.

Liliana Perez and Suzana Dragicevic. 2009. An agent-based approach for modeling dynamics of contagious disease spread. *International journal of health geographics* 8, 1 (2009), 1–17.

Meirui Qian and Jianli Jiang. 2020. COVID-19 and social distancing. *Journal of Public Health* (2020), 1–3.

Parveena Samim Abdul Salam, Wolfgang Bock, Axel Klar, and Sudarshan Tiwari. 2021. Disease contagion models coupled to crowd motion and mesh-free simulation. *arXiv preprint arXiv:2101.01598* (2021).

Md Salman Shamil, Farhanaz Farheen, Nabil Ibtehaz, Irtesam Mahmud Khan, and M Sohel Rahman. 2021. An agent-based modeling of COVID-19: validation, analysis, and recommendations. *Cognitive Computation* (2021), 1–12.

ATRB Skvortsov, RB Connell, P Dawson, and R Gailis. 2007. Epidemic modelling: Validation of agent-based simulation by using simple mathematical models. In *Proceedings of Land Warfare Conference*, Vol. 2007. Citeseer, 221–227.

Daniel Thalmann, Carol O'Sullivan, Barbara Yersin, Jonathan Maim, and Rachel McDonnell. 2007. EG 2007 Course on Populating Virtual Environments with Crowds.. In *Eurographics (Tutorials)*. 23–123.

Jur Van den Berg, Ming Lin, and Dinesh Manocha. 2008. Reciprocal velocity obstacles for real-time multi-agent navigation. In *2008 IEEE International Conference on Robotics and Automation*. IEEE, 1928–1935.

Wouter van Toll, Thomas Chatagnon, Cédric Braga, Barbara Solenthaler, and Julien Pettré. 2021. SPH crowds: Agent-based crowd simulation up to extreme densities using fluid dynamics. *Computers & Graphics* (2021).

Patrick Walker, Charles Whittaker, Oliver Watson, Marc Baguelin, K Ainslie, Sangeeta Bhatia, Samir Bhatt, A Boonyasiri, O Boyd, L Cattarino, et al. 2020. Report 12: The global impact of COVID-19 and strategies for mitigation and suppression. (2020).

Xueying Wang, Drew Posny, and Jin Wang. 2016. A reaction-convection-diffusion model for cholera spatial dynamics. *Discrete & Continuous Dynamical Systems-B* 21, 8 (2016), 2785.

Tomer Weiss, Alan Litteneker, Chenfanfu Jiang, and Demetri Terzopoulos. 2019. Position-based real-time simulation of large crowds. *Computers & Graphics* 78 (2019), 12–22.

Christopher Wolfram. 2020. An agent-based model of covid-19. *Complex Systems* 29, 1 (2020), 87–105.

Yanni Xiao and Lansun Chen. 2001. Modeling and analysis of a predator–prey model with disease in the prey. *Mathematical biosciences* 171, 1 (2001), 59–82.

Mingliang Xu, Xiaozheng Xie, Pei Lv, Jianwei Niu, Hua Wang, Chaochao Li, Ruijie Zhu, Zhigang Deng, and Bing Zhou. 2019. Crowd behavior simulation with emotional contagion in unexpected multihazard situations. *IEEE Transactions on Systems, Man, and Cybernetics: Systems* (2019).

Ping Xu and Jiuqing Cheng. 2021. Individual differences in social distancing and mask-wearing in the pandemic of COVID-19: The role of need for cognition, self-control and risk attitude. *Personality and individual differences* 175 (2021), 110706.

Tao Xue, Xiaobing Zhang, and Kumar K Tamma. 2019. A non-local dissipative Lagrangian modelling for generalized thermoelasticity in solids. *Applied Mathematical Modelling* 73 (2019), 247–265.

Kazuo Yamazaki and Xueying Wang. 2017. Global stability and uniform persistence of the reaction-convection-diffusion cholera epidemic model. *arXiv preprint arXiv:1701.01407* (2017).